





Peptide self-assembly as a strategy for facile immobilization of redox enzymes on carbon electrodes

Itzhak Grinberg^{1,2,3}  | Oren Ben-Zvi⁴  | Lihi Adler-Abramovich^{1,2,3}  | Iftach Yacoby⁴ 

¹Department of Oral Biology, The Goldschleger School of Dental Medicine, Faculty of Medicine, Tel Aviv University, Tel Aviv, Israel

²The Center for Nanoscience and Nanotechnology, Tel Aviv University, Tel Aviv, Israel

³The Center for the Physics and Chemistry of Living Systems, Tel Aviv University, Tel Aviv, Israel

⁴School of Plant Sciences and Food Security, The George S. Wise Faculty of Life Sciences, Tel Aviv University, Tel Aviv, Israel

Correspondence

Lihi Adler-Abramovich, Department of Oral Biology, The Goldschleger School of Dental Medicine, Faculty of Medicine, Tel Aviv University, Tel Aviv 6997801, Israel.

Email: LihiA@tauex.tau.ac.il

Iftach Yacoby, School of Plant Sciences and Food Security, The George S. Wise Faculty of Life Sciences, Tel Aviv University, Tel Aviv 6997801, Israel.

Email: iftachy@tauex.tau.ac.il

Funding information

Ministry of Energy, Israel, Grant/Award Numbers: 219-11-120, 222-11-065; Israel Science Foundation, Grant/Award Number: GA 2185/17

Abstract

Redox-enzyme-mediated electrochemical processes such as hydrogen production, nitrogen fixation, and CO₂ reduction are at the forefront of the green chemistry revolution. To scale up, the inefficient two-dimensional (2D) immobilization of redox enzymes on working electrodes must be replaced by an efficient dense 3D system. Fabrication of 3D electrodes was demonstrated by embedding enzymes in polymer matrices. However, several requirements, such as simple immobilization, prolonged stability, and resistance to enzyme leakage, still need to be addressed. The study presented here aims to overcome these gaps by immobilizing enzymes in a supramolecular hydrogel formed by the self-assembly of the peptide hydrogelator fluorenylmethyloxycarbonyl-diphenylalanine. Harnessing the self-assembly process avoids the need for tedious and potentially harmful chemistry, allowing the rapid loading of enzymes on a 3D electrode under mild conditions. Using the [FeFe] hydrogenase enzyme, high enzyme loads, prolonged resistance against electrophoresis, and highly efficient hydrogen production are demonstrated. Further, this enzyme retention is shown to arise from its interaction with the peptide nanofibrils. Finally, this method is successfully used to retain other redox enzymes, paving the way for a variety of enzyme-mediated electrochemical applications.

KEYWORDS

3D electrode, enzymes encapsulation, H₂ production, hydrogenase, peptide hydrogel

Itzhak Grinberg and Oren Ben-Zvi contributed equally to this work.

This is an open access article under the terms of the Creative Commons Attribution License, which permits use, distribution and reproduction in any medium, provided the original work is properly cited.

© 2023 The Authors. *Carbon Energy* published by Wenzhou University and John Wiley & Sons Australia, Ltd.

1 | INTRODUCTION

Molecular hydrogen (H_2) is a valuable commodity for both the chemical industry and the energy market. However, H_2 is not naturally abundant and has to be produced. Most commonly, fossil fuels are used to create “gray” H_2 , which is considered unsustainable in the carbon-neutral future. Alternatively, the carbon-neutral “green” H_2 is currently produced by water electrolysis, powered by renewable energy sources such as solar and wind. While water electrolysis technologies have greatly progressed in recent years, this process still faces inherent limitations such as a thermodynamic minimum potential difference of 1.23 V and overpotential issues.^{1–3} A different approach for H_2 production is the utilization of a biocatalyst. Enzymes possess a variety of advantages as biocatalysts, including negligible overpotential, high specificity, and complete biodegradability.⁴ Hence, enzymes can catalyze chemical reactions in a high-yield, scalable cost-efficient manner and under mild conditions. Hydrogenases, H_2 -producing enzymes, are a diverse group of metalloenzymes that catalyze both the reduction of protons into H_2 and the reverse reaction.⁵ The direction of catalysis is influenced by the metallic cofactor at the enzyme catalytic site, where [FeFe] hydrogenases are typically more suitable for H_2 production, while [NiFe] hydrogenases tend to favor H_2 oxidation.⁶ The reduction of protons to H_2 at the [FeFe] hydrogenase active site requires redox potentials ranging between -0.37 and -0.45 V under physiological conditions, depending on the specific hydrogenase species and the pH.⁷ Since these potentials are significantly lower than the 1.23 V required for water splitting, hydrogenases are considered promising biocatalysts. In addition, the active site of hydrogenases is situated near the enzyme surface, and is therefore suitable for direct electron transfer,^{8–10} that is, a direct electronic communication between the active site and the electrode surface. For this communication to occur, enzymes must be tethered onto a conductive surface in the correct orientation to permit direct electron transfer between the surface and the biomolecule. This can be achieved using several methods, ranging from simple absorption^{11,12} to electrode functionalization^{13,14} and sophisticated cross-linking strategies,^{15,16} with significant progress made in this field.¹⁷ However, direct electron transfer is limited by the two-dimensional (2D) planar nature of the electrodes, namely, the total amount of enzyme, and therefore, the overall activity is limited by the electrode surface area. Alternatively, enzymes can be powered by mediated electron transfer, in which the electrons are shuttled to an unbound enzyme by a mediator. In the case of hydrogenases, methyl viologen (MV), a common organic

dye with a redox potential of -0.44 V, is often used for this purpose.^{18–20}

In its simplest form, the mediated electron transfer technique is applied in the bulk volume of the electrochemical cell, although very inefficiently.²¹ Another method uses casting of the enzyme and mediator on an electrode surface. The mediator can either be freely diffused or covalently linked to a polymer (redox polymer), in which the enzyme is embedded. Such redox polymers were successfully demonstrated to activate hydrogenases by using MV²² and cobaltocene mediators.²³ Although this method presumably removes the surface limitation, it is currently limited by the small volume and the planar conductive surface. Increasing the thickness of materials cast on the electrode adds distance between the conductive surface and the catalyst, and is therefore hindered by limited diffusion of the mediator.^{24,25} The surface limitation of planar electrodes in both direct and mediated electron transfer settings prompts researchers to study ways to increase the available surface area. This is usually achieved by the fabrication of an electrode with a 3D architecture, which allows loading of more active material, compared to planar electrodes. Such electrodes can be made of an inorganic compound as was demonstrated with a hierarchically structured indium–tin oxide electrode,^{26,27} or carbon-based materials that are considered ideal scaffolds for this purpose.²⁸ Indeed, hydrogenases were successfully bound to pyrolytic graphite²⁹ and carbon nanotubes³⁰ to fabricate 3D-hydrogenase electrodes for direct electron transfer. A mediated electron transfer approach that makes use of a 3D-enzymatic electrode requires immobilization of the enzyme in proximity to the electrode.²¹ Such immobilization prevents diffusion of enzyme molecules away from the electrode, and the subsequent significant reduction in its efficiency. Immobilization on an electrode may be achieved by noncovalent methods such as physical entrapment, physical adsorption, and encapsulation in polymer-based matrices.^{31,32} Specifically, vinylpyrrolidone was used to entrap [NiFe] hydrogenase in a carbon felt electrode.³³ However, embedding enzymes in polymer matrices could be a tedious process, which might require chemical modifications, voltage application, and washing and drying steps, all of which may have a negative effect on the enzyme activity. Additionally, these methods often require harsh conditions, such as high temperatures or extreme pH, which can further compromise the protein integrity, thus requiring careful planning.³⁴ These constraints can be avoided with the use of self-assembled peptide-based hydrogels, which spontaneously form under mild conditions and offer an attractive alternative approach for protein immobilization.^{35,36}

Peptide-based hydrogels are environmentally friendly, easily synthesized, soft, and biocompatible materials, which mainly consist of aqueous content.³⁷ Supramolecular self-assembly serves as a key approach for the formation of such bulk hydrogels; thus, low-molecular-weight hydrogelators have been widely explored.^{38–43} Self-assembly can be triggered by a change in the conditions, that is, pH³⁹ or solvent switch,³⁸ or assisted by enzymatic activity that can facilitate localized self-assembly.^{44,45} However, there may be some limitations to their use, such as potential difficulties in controlling the structure of the hydrogel or its stability over time.^{46,47} In addition, the performance of the hydrogel may depend on the specific peptides used and the conditions under which they are assembled.⁴⁸ A notable example of a peptide-based hydrogelator is fluorenylmethoxycarbonyl-diphenylalanine (FmocFF), an aromatic dipeptide building block that can self-assemble in aqueous solutions into nanoscale ordered fibrils, which form a 3D hydrogel network.^{40,41,49} Self-assembly of FmocFF is stabilized by π - π interactions between the aromatic rings of the peptide molecules.^{50–53}

It was shown that the FmocFF hydrogel stably retains proteins of over 5 kDa, while smaller molecules are less restricted.⁴⁰ In this regard, we have previously demonstrated that [FeFe] hydrogenase can be chemically activated by the small soluble MV while encapsulated in the FmocFF hydrogel.⁵⁴

Herein, we describe an enzyme encapsulation approach allowing facile and robust immobilization of *Chlamydomonas reinhardtii* [FeFe] hydrogenase (HydA) on a carbon felt electrode, utilizing the self-assembly of the peptide hydrogelator FmocFF. We demonstrate the high capacity of the FmocFF assembly to stably retain proteins on its nanofibrils, while also accumulating over the carbon fibers. Our system relies on electron transfer mediated by MV, which is reduced at the carbon fibers and shuttles the electrons to the encapsulated enzyme, to be used for the production of H₂. This immobilization approach allows us to simultaneously take advantage of the carbon felt 3D architecture to maintain efficient electron shuttling, overcoming the surface limitation to encapsulate protein at high amounts, under mild conditions, and with relative ease and stability.

2 | EXPERIMENTAL

2.1 | Materials

FmocFF was purchased from Bachem. Fmoc-leucine-leucine (FmocLL) was purchased from GL Biochem. Dimethyl sulfoxide (DMSO) ReagentPlus[®] $\geq 99.5\%$, MV

dichloride hydrate 98%, and sodium dithionite, technical grade 85%, were purchased from Sigma-Aldrich. Tris (hydroxymethyl)aminomethane (Tris) was purchased from Bio-Lab Ltd. SIGRACELL[®] GFD 4.65 EA carbon felt was purchased from SGL Carbon, with a stated thickness of 4.6 mm, density of 0.09 g/cm³, porosity of 94%, brunauer-emmett-teller surface area of 0.4 m²/g, longitudinal electrical resistivity of <5 Ω mm, and transverse electrical resistivity of <3 Ω mm. The diameter of individual carbon fibers was measured by us in scanning electron microscopy (SEM) images as $\sim 9 \mu\text{m}$. [FeFe] Hydrogenase, Fe superoxide dismutase (SOD), and ferredoxin-NADP⁺ reductase (FNR) enzymes were expressed and purified inhouse according to published protocols.^{55–57} Rabbit polyclonal *C. reinhardtii* HydA1/2, SOD, and FNR primary antibodies were purchased from Agrisera. Cyanine5 (Cy5) NHS ester was purchased from Lumiprobe.

2.2 | Electrode preparation

Electrode fabrication was conducted in an anaerobic chamber (3.5% H₂ balance N₂, Coy Laboratories). Tris-HCl pH 7.2 buffered solution was supplemented with 1 mM sodium dithionite, 2 mM MV, and HydA enzyme, while peptide hydrogelator powder was dissolved in DMSO to a concentration of 100 mg mL⁻¹. The two solutions were then mixed and immediately soaked on a 2 × 1 cm carbon felt, followed by a 2-h gelation period. For FmocFF electrodes, a final concentration of 35% DMSO and 80 mM Tris-HCl pH 7.2 was used to allow sufficient soaking time due to rapid gelation in buffered solution.⁴⁴ FmocLL electrodes were prepared at a final concentration of 10% DMSO, 80 mM Tris-HCl pH 7.2. For solution-soaked electrodes, only 80 mM Tris-HCl pH 7.2 buffer was used. Unless stated otherwise, all electrodes contained 200 μg of HydA enzyme, while 5 mg of peptide hydrogelator was used in either FmocFF or FmocLL electrodes.

2.3 | Electrochemical measurements

Cyclic voltammetry and chronoamperometry were performed using a MultiPalmSens4 (Palm Sense) potentiostat with three-electrode configuration cells. All experiments were carried out in a custom-made 100 mL electrochemical cell fitted with a sample valve for headspace purging and measurements. The electrochemical cell was filled with 50 mL of electrolyte (100 mM Tris-HCl pH 7.2, 100 mM KCl) at room temperature. A carbon felt working electrode was threaded onto a

platinum wire in an anaerobic environment and transferred to the electrolytic cell. An RE-1S Ag/AgCl electrode (ALS Co.) and a platinum mesh were used as the reference and counter electrodes, respectively. All electrodes were wired to the top stopper of the electrochemical cell while submerged in electrolyte solution. Prior to experiment onset, the cell headspace was purged with argon gas for 10 min. The scan rate for cyclic voltammetry was 50 mV/s in a range of -0.8 to 0.4 V versus standard hydrogen electrode (SHE). The potential for chronoamperometry was set at -0.6 V versus SHE for a duration of 18 h. H_2 gas was measured by sampling the cell headspace using a Hewlett-Packard 5890 Series II gas chromatograph (Agilent Technologies).

2.4 | HydA enzymatic activity measurement

Carbon felt electrodes were prepared as described above (Figure 1). In addition, samples were subjected to 1 h washing in 50 mL of electrolyte per electrode to remove DMSO traces. Following washing, fresh samples were assayed immediately, while other tested samples were incubated for 18 h under different conditions: aged samples were removed into dry 7 mL septum-sealed serum glass vials (Wheaton), immersed samples were left in the electrolyte without further procedures, and electrochemically activated samples were subjected to a constant potential of -0.6 V versus SHE in an electrochemical cell. HydA activity determination was then conducted by placing the carbon felt electrodes in 7 mL of septum-sealed serum glass vials under anaerobic conditions, while purging with argon gas for 10 min, and supplementing the vials with 1 mL of activity buffer (100 mM Tris-HCl pH 7.2, 1 M NaCl, 20 mM sodium dithionite, and 10 mM MV). The vials were then incubated at 50°C in a water bath, while 500 μL of headspace gas samples were drawn at 6-min intervals. The concentration of H_2 in the vial headspace was measured using a Hewlett-Packard 5890 Series II gas chromatograph (Agilent Technologies). The residual activity of HydA was determined by comparing the samples to the corresponding fresh control.

2.5 | Immunoblot

The electrolyte from the electrolytic cell was collected following 18-h chronoamperometry and concentrated 100-fold using an Amicon[®] Ultra 15 mL centrifugal device, with a cutoff of 10,000 Da (Merc). Equal volumes of electrolyte were incubated for 10 min at 72°C with Bolt

LDS sample buffer (Invitrogen). Samples were then loaded on 4–12 Bis-Tris Plus PAGE gels[®] (Invitrogen) and analyzed by immunoblotting using the iBind blotter and its specific blocking reagents[®] (Invitrogen). Rabbit polyclonal HydA1/2, SOD, and FNR antibodies were used as the primary antibodies. Membrane images were taken using an Amersham ImageQuant 800 station (Cytiva).

2.6 | Rheology

Rheology measurements were carried out using an AR-G2 controlled-stress rheometer (TA Instruments). To determine the linear viscoelastic region, oscillatory strain (0.01%–100%) and frequency sweep (0.01–100 Hz) tests were performed in parallel plate geometry. The hydrogels were prepared by pipetting Tris buffer (100 mM, pH 7.2) onto FmocFF solution in DMSO, reaching final FmocFF concentrations of 1–5 mg mL⁻¹ and a final DMSO concentration of 35%, and immediately dropping 250 μL of the mixture onto the rheometer plate. The geometry was immediately set at a gap size of 600 μm , and a 2-h soak time was allowed before measurement onset. Time sweep oscillatory tests were performed for 5 h at a constant frequency of 1 Hz and strain of 0.1% to determine G' and G'' , the storage and loss moduli, respectively. All measurements were conducted at room temperature.

2.7 | Scanning electron microscopy

Carbon felt electrodes were prepared as described above, followed by 1 h washing with 50 mL of Tris-HCl buffer (100 mM, pH 7.2) per electrode to remove DMSO traces. To obtain cross section views of the electrode interior, samples were flash-frozen in liquid nitrogen before being fragmented. Samples were freeze-dried, and Au sputter coating of dried samples was performed before imaging in a JEOL JSM-IT 100 SEM (JEOL) operating at 20 kV.

2.8 | Confocal microscopy

Proteins were diluted in phosphate buffer (100 mM, pH 8) to 1 mg mL⁻¹. Cy5 NHS ester was dissolved in dimethylformamide (DMF) and added to the protein solution at a 3:1 molar ratio, while maintaining the final concentration of DMF at 10%. The solution was shaken overnight at 4°C , and then DMF, buffer, and excess dye were washed with Tris-HCl buffer (100 mM, pH 7.2) using a 10,000 Da cutoff Amicon[®] Ultra 15 mL centrifugal device. Samples of carbon felt electrode containing stained protein were prepared as

described above. Hydrogel samples containing stained proteins were prepared in a similar manner but without carbon felt. Imaging was performed using a ZEISS LSM 900 confocal microscope (ZEISS).

3 | RESULTS AND DISCUSSION

3.1 | Encapsulating HydA in an FmocFF peptide hydrogel soaked on carbon felt maintains stable and reproducible electron transfer

Electrode preparation was conducted in an anaerobic chamber. Tris-HCl pH 7.2 buffered solution was supplemented with MV and HydA enzyme and mixed with a DMSO solution of the peptide hydrogelator. Notably, rapid initiation of gelation necessitated immediate soaking of the mixture onto the carbon felt. Self-assembly was allowed to occur for 2 h. The electrodes were then tethered on a platinum wire and placed in an

electrochemical cell (Figure 1). The FmocFF hydrogels were compared to another self-assembling peptide gelator, FmocLL (Figure 2). To study the electrochemical properties of the electrode-containing carbon felt soaked with MV, FmocFF, and active HydA enzyme, we performed cyclic voltammetry measurements (Figure 3A,B). The combination of the FmocFF hydrogel with both MV and HydA produced a strong reduction peak, reaching a current of 3.5 mA at -0.54 V, attributed to the reduction of MV^{+2} (MV^{ox}) to MV^+ (MV^{red}) (Figure 3A[I]). An oxidation peak was detected at -0.33 V as the MV^{red} pool was oxidized back to MV^{ox} (Figure 3A[II]), followed by a sustained current of 1 mA between -0.2 and 0.4 V. This observation may be due to H_2 gas, produced by HydA during the reduction phase, being oxidized by the reverse reaction of the enzyme, which reduces MV^{ox} to MV^{red} . Subsequently, MV^{red} was oxidized at the electrode, resulting in the measured current between -0.2 and 0.4 V (Figure 3A[III]). To further understand the contribution of each component of the electrode, we studied the electrochemical

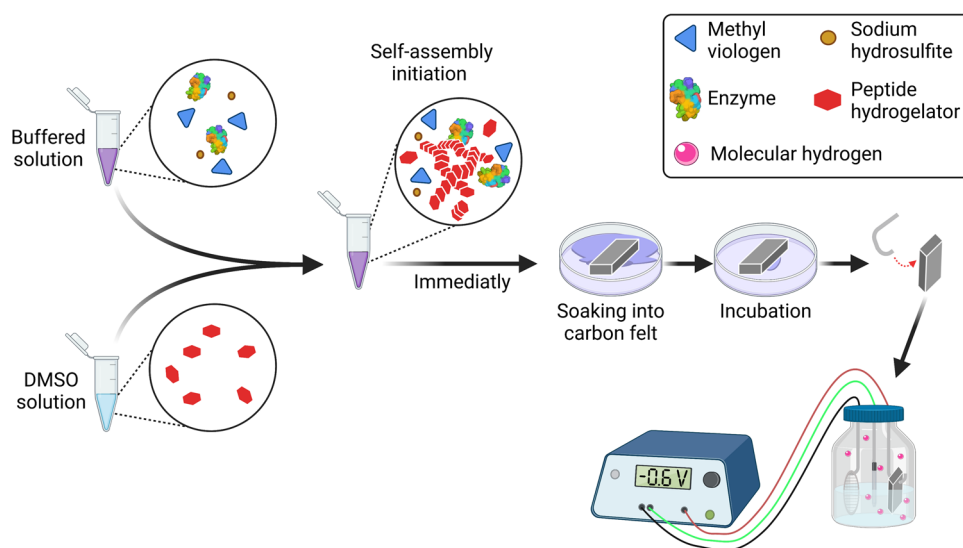


FIGURE 1 Schematic diagram of electrode preparation.

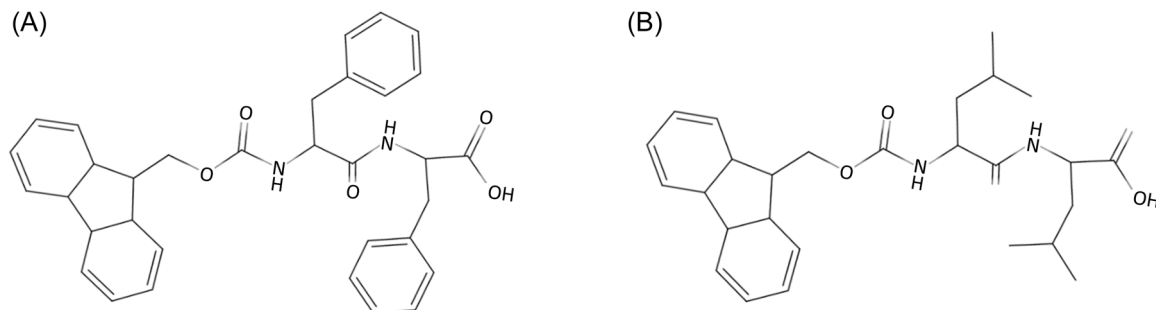


FIGURE 2 Molecular structure of the peptide hydrogelators. (A) FmocFF and (B) FmocLL.

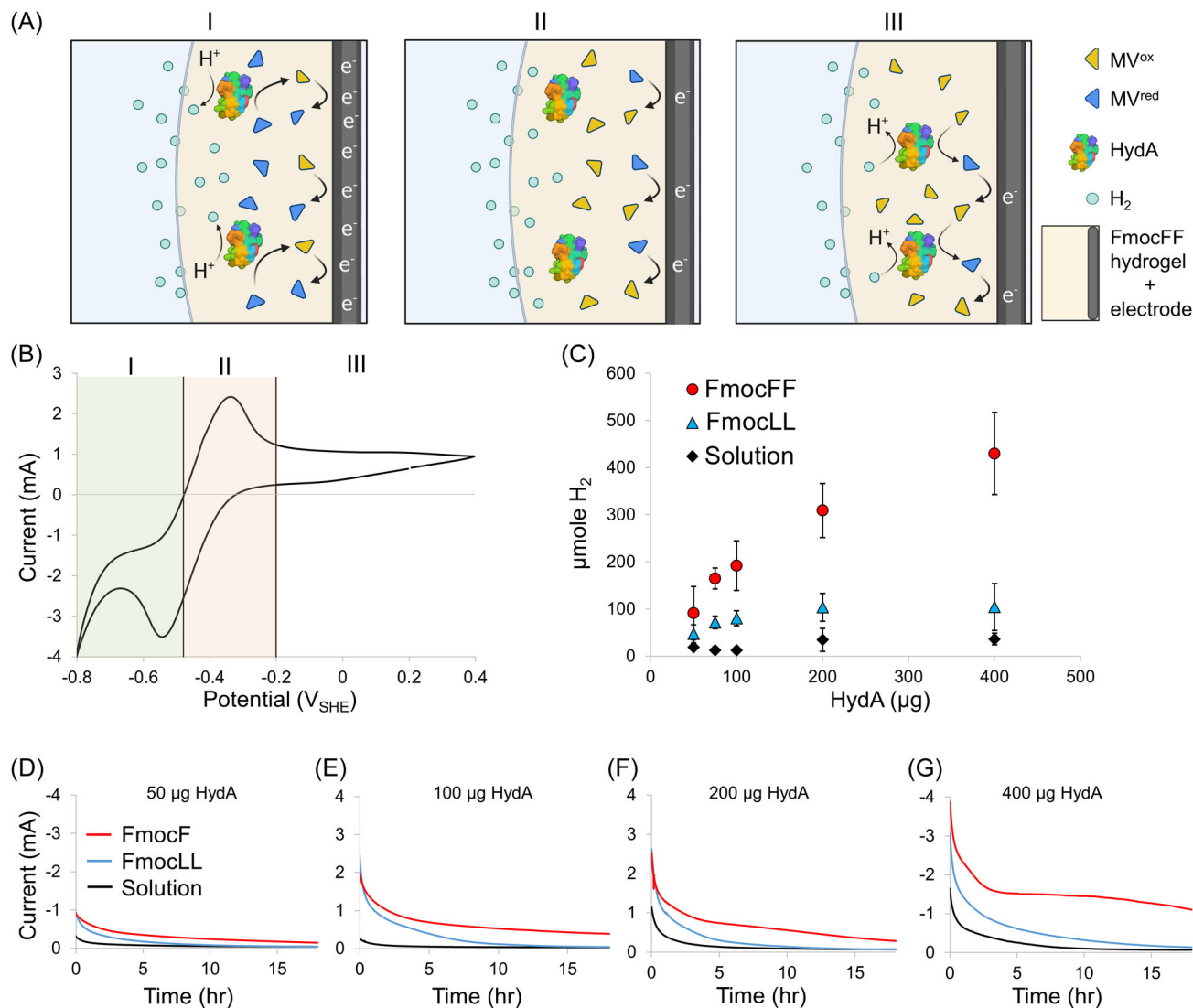


FIGURE 3 Electrochemical properties of HydA encapsulated in an FmocFF-soaked electrode. (A) Proposed scheme of the electrochemical activity at different potentials. Yellow triangles represent MV^{ox}, blue triangles represent MV^{red}, HydA is represented by its protein crystallographic structure, light blue circles represent H₂, and the dark-gray and light-yellow areas, respectively, represent the carbon felt electrode soaked with the FmocFF hydrogel. I. Reduction of MV by the electrode and shuttling of electrons to HydA, which catalyzes H₂ production. II. Oxidation of the MV pool at the electrode. III. H₂ oxidation by HydA reduces MV, which shuttles the electrons back to the electrode. (B) Cyclic voltammogram of the FmocFF hydrogel soaked on a carbon felt electrode supplemented with HydA and MV. (C) Accumulated H₂ produced overnight (O.N.) by the electrochemical assay versus the amount of enzyme loaded on the working electrode in the FmocFF hydrogel (red circles), the FmocLL hydrogel (blue triangles), and the solution (black diamonds). Error bars represent mean ± SD of at least six independent experiments. (D–G) Corresponding chronoamperometries of O.N. electrochemical assays of FmocFF-, FmocLL-, and solution-soaked electrodes (red, blue, and black, respectively).

properties for the following combinations: (i) carbon felt soaked with MV and FmocFF in the absence of an active HydA enzyme (Figure S1), (ii) carbon felt soaked with FmocFF and active HydA without MV (Figure S2), and (iii) carbon felt soaked with only the FmocFF hydrogel (Figure S3). Indeed, the FmocFF hydrogel with MV alone (i) yielded a similarly cyclic voltammogram, but without any detectable current following MV oxidation at -0.33 V (Figure S1).

These observations demonstrate the mobility of MV in the FmocFF hydrogel as it readily carried electrons to and from the biocatalyst. We also found that carbon felt soaked with FmocFF and the active HydA enzyme, without the presence of MV (ii), did not produce a notable current, showing only a minor reduction peak at -0.45 V. This is in line with the known redox potential of the HydA active site⁵⁵ (Figure S2). Hence, while some direct electron transfer does occur, most of the

encapsulated enzyme is too distant from the electrode surface. Hence, the utilization of the electrode's full potential requires an electron mediator. Finally, as expected, carbon felt soaked with the FmocFF hydrogel alone (iii) produced no peaks throughout the range of -0.8 to 0.4 V vs. SHE (Figure S3).

3.2 | The FmocFF hydrogel permits high enzyme load and utilization at high faradaic efficiency

To test the ability of the FmocFF hydrogel to entrap the HydA enzyme in a carbon felt electrode, different concentrations of the enzyme were loaded while the size of the carbon felt electrode and the hydrogel volume were kept constant. The samples were prepared in an anaerobic environment and placed as a working electrode in a three-electrode electrochemical cell. Chronoamperometry was recorded overnight at -0.6 V SHE, and the cell headspace was sampled to quantify the total H_2 production following 18 h of potential application. We observed that increasing the concentrations of HydA in carbon felt electrodes, in the absence of a hydrogel matrix, failed to result in increased H_2 production due to enzyme diffusion out of the electrode (Figure 3C). Encapsulation of HydA in the FmocLL-soaked electrode produced a mild improvement in the total H_2 production, but not in a concentration-dependent manner. In contrast, H_2 production was in direct correlation to the concentrations of HydA encapsulated in the FmocFF-soaked carbon felt electrode. The accumulated H_2 increased from 90 to 430 μmol as the quantity of the HydA enzyme was increased from 50 to 400 μg (Figure 3C). Furthermore, the recorded chronoamperometry of FmocFF-soaked electrodes showed a relatively stable current profile with a mild current decay and higher currents for higher enzyme concentrations. Notably, the observed current following 18 h was sufficient to produce visible bubbling of H_2 from the electrode. In contrast, the solution-soaked electrodes showed a low current immediately upon voltage application, which continued to decline until voltage termination. As for the FmocLL-soaked carbon felt, the currents recorded were similar to those of FmocFF in the first 10 min; however, as the measurements continued, a strong decay of the current was observed, which resulted in complete reaction cessation after ~ 10 h at all enzyme concentrations (Figure 3D–G). The relatively stable enzymatic activity in the FmocFF hydrogel, as observed by chronoamperometry, suggests a strong enzyme-encaging ability. Hence, soaking the carbon felt with the FmocFF hydrogel allowed us to retain a higher

concentration of the enzyme in proximity to the electrode. Indeed, H_2 production yields in the FmocFF hydrogel increased with the enzyme concentration due to the higher overall enzymatic activity. In contrast, the complete decay of the current in the FmocLL hydrogel suggests a weak retention ability, which is further supported by its inability to achieve higher H_2 production with a high enzyme concentration (Figure 3C), likely since excess enzyme diffuses out of the electrode. The difference between the two peptide hydrogels is intriguing, as both have similar chemical and assembly properties and form hydrogels with a nanofibrillar structure, with FmocLL shown to increase the stability of an [FeFe] hydrogenase model compound.⁵⁶ Finally, by integrating the area under the current curve for the total charge (Figure 3D–G) and considering the moles of H_2 that were produced (Figure 3C), the Faradaic efficiency was calculated and found to be $\sim 80\%$ – 90% for all the tested conditions. This high efficiency can be attributed to the high specificity of the enzymatic reaction. Still, the relatively low Faradaic loss indicates some unwanted side reactions, for example, O_2 reduction into O_2^- by MV^{red} . O_2 may be introduced into the system via minor air leaks.

3.3 | Encapsulation in FmocFF modulates the enzyme distribution in carbon-felt electrodes

To investigate the mode of enzyme encaging by the peptide hydrogels within the carbon felt electrode, we performed confocal microscopy analysis. Carbon felt electrodes were prepared using HydA covalently linked to the fluorescent dye Cy5. Figure 4A–C shows the carbon felt fibers as visualized via bright field as well as the localization of the enzyme within the electrode as detected via fluorescence microscopy for samples of dyed HydA in buffer solution, FmocFF-encapsulated and FmocLL-encapsulated. Notably, neither pristine FmocFF nor FmocLL fibrils showed fluorescence in the tested wavelengths; therefore, the detected fluorescence was attributed to the dyed enzyme. Interestingly, while the enzyme encapsulated in the FmocLL hydrogel appeared to be arranged into clumps in between the carbon fibers (Figure 4B), the enzyme encapsulated in FmocFF was concentrated directly on the carbon felt fibers (Figure 4C). This arrangement holds potential in overcoming limitations of mediator diffusion due to the short distance between the enzyme and the electrode surface. Inspecting the solution-soaked carbon felt revealed no fluorescence signal, most likely due to the enzyme not being concentrated in a certain location, but rather evenly distributed throughout the sample (Figure 4A).

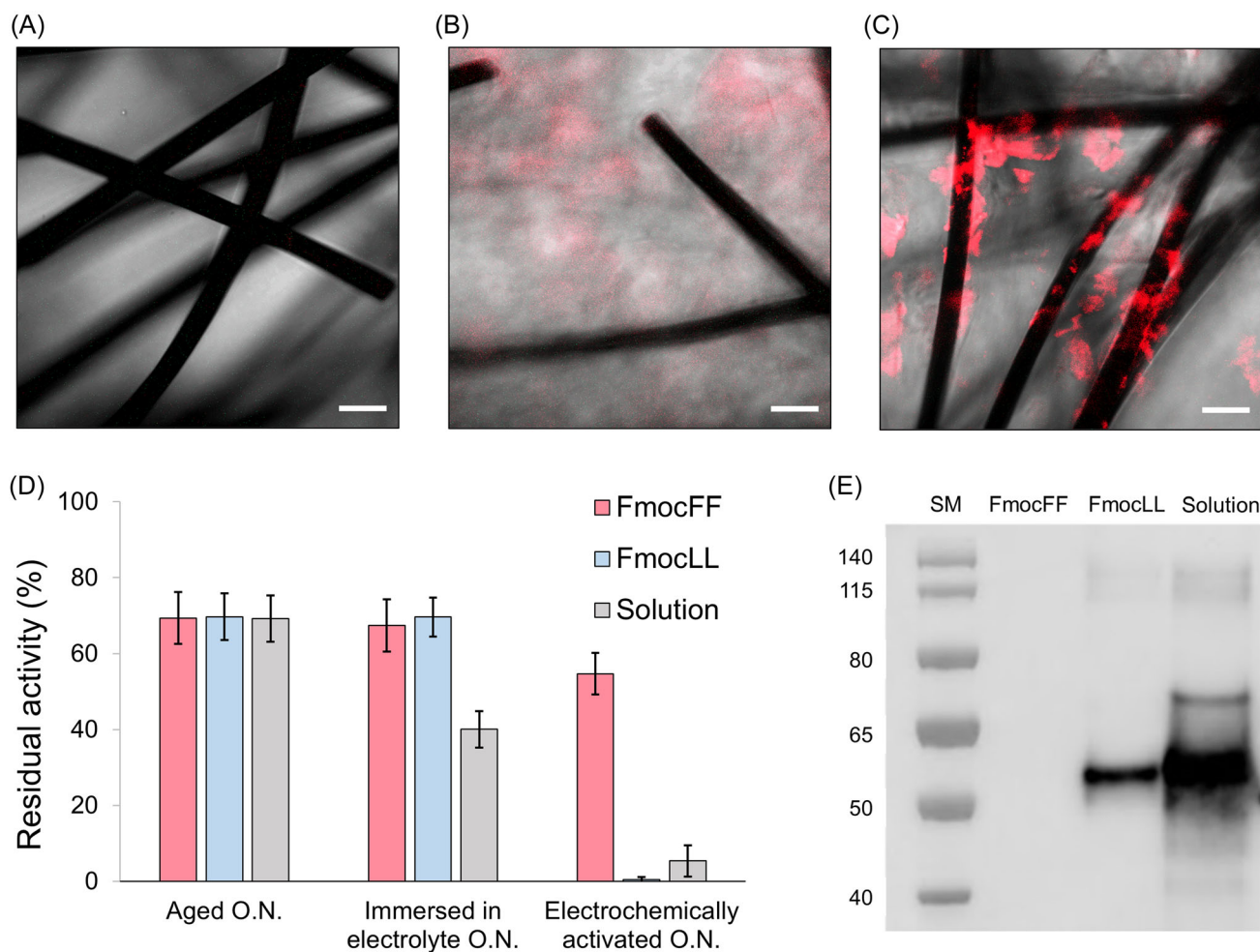


FIGURE 4 Enzyme distribution and retention on the electrode. (A–C) Overlaid confocal images of fluorescent Cy5-stained HydA enzyme, soaked on carbon felt (viewed in bright field); the scale bar is 20 μm . (A) HydA in solution. (B) HydA encapsulated in the FmocLL hydrogel. (C) HydA encapsulated in the FmocFF hydrogel. (D) Residual activity of HydA soaked on carbon felt in either the FmocFF hydrogel, the FmocLL hydrogel, or solution, subjected to either overnight (O.N.) aging, immersion in electrolyte solution, or electrochemical activation. Error bars represent mean \pm SD of at least six independent experiments. (E) Immunoblot of HydA in the electrolyte collected after O.N. electrochemical activation in the FmocFF hydrogel, the FmocLL hydrogel, or solution.

This difference in morphology may indicate a difference in the ability to retain the enzyme within the carbon felt electrode. However, this does not rule out a different mechanism, not related to the retention ability.

3.4 | FmocFF hydrogel encapsulation prevents enzyme electrophoresis

To elucidate the decline in H_2 production over time, we tested whether the enzyme was slowly inactivated or rather diffused out of the carbon felt. We performed a chemical assay measuring the residual activity of HydA soaked in the carbon felt, with and without hydrogel encapsulation. Samples of 75 μg HydA were used in (i) solution-soaked carbon felt, (ii) FmocLL hydrogel-soaked carbon felt, and (iii)

FmocFF hydrogel-soaked carbon felt. Fresh samples were assayed immediately to establish the activity baseline for each group. To investigate a possible aging effect, samples were placed in sealed vials overnight and then the innate loss of activity, if any, was measured. Overnight aging resulted in a 30% loss of activity regardless of the encapsulation method, suggesting that the enzyme is stable in the peptide hydrogels as no specific loss of activity was observed (Figure 4D). Hence, enzyme stability cannot account for the difference observed in the electrochemical assay. To test for passive diffusion of the enzyme out of the electrode and into the electrolyte, the samples were immersed in an electrolyte solution overnight. We found that when immersed in electrolyte solution, both hydrogels showed the same activity as the aged samples, while the solution-soaked electrodes lost an additional 30% of activity (60% in total) (Figure 4D).

To investigate the possible role of electrophoresis, another group of samples was subjected to steady electrical voltage during an overnight electrochemical H_2 production experiment. We observed that while the residual enzymatic activities of both FmocLL and solution samples were extremely low, the samples encapsulated in FmocFF retained 55% of the HydA activity, compared to fresh samples (Figure 4D). These observations imply that both hydrogels successfully prevented the enzyme from passively diffusing out. However, a significant difference between the two hydrogels was observed when the samples were subjected to overnight electrochemical activation. These results are in accordance with the chronoamperometry analysis shown in Figure 3C and the corresponding H_2 produced.

The loss of HydA activity in the FmocLL hydrogel can be attributed to either inactivation of the encapsulated enzyme or electrophoresis of active protein out of the hydrogel. To distinguish between these options, we collected the electrolyte solution from the electrochemical cells, concentrated it, and analyzed it using an immunoblot assay using specific anti-HydA antibodies to detect leaked enzyme. Figure 4E shows a notable protein band detected using the electrolyte sample from the cell comprising either solution-soaked electrode or the FmocLL hydrogel

electrode, indicating high levels of leaked protein. Remarkably, no protein was detected in the electrolyte surrounding the FmocFF-soaked electrode (Figure 4E). This implies that protein electrophoresis is the prominent factor limiting H_2 production in both the solution and FmocLL hydrogel samples. Thus, the retention of HydA in the FmocFF hydrogel, even under an electric field, presumably supports the prolonged function of the hydrogel-soaked electrode.

3.5 | Enzyme retention by FmocFF assemblies is independent of gel state

To understand whether the formation of a gel is a prerequisite for the encapsulation and activity of HydA in our electrochemical system, we soaked carbon felt electrodes with FmocFF at a concentration range of $1\text{--}5\text{ mg mL}^{-1}$. It is noteworthy that increasing FmocFF concentration resulted in shorter gelation times (Figure S4). This gelation kinetics presented a technical difficulty for the fabrication of FmocFF-soaked electrodes with concentrations exceeding 5 mg mL^{-1} , as a liquid state of at least $5\text{--}10\text{ s}$ is required for complete absorption into the carbon felt electrode.

As shown in the tilted tubes in Figure 5A, a liquid suspension of self-assembled fibrils, rather than a

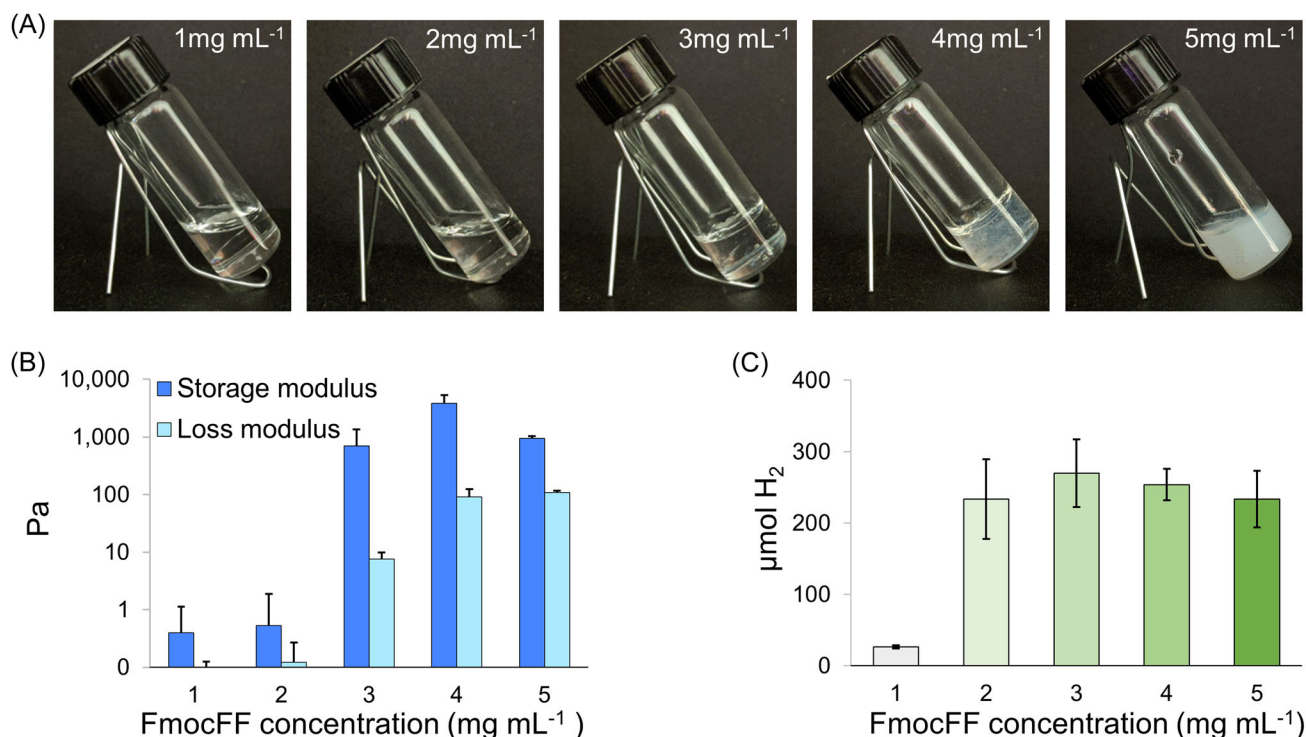


FIGURE 5 Effect of the FmocFF concentration on hydrogel properties and electrode activity. (A) Tilted vials of FmocFF at concentrations of $1\text{--}5\text{ mg mL}^{-1}$. (B) Rheology of FmocFF at concentrations of $1\text{--}5\text{ mg mL}^{-1}$. (C) Accumulated H_2 after overnight electrochemical activation of the HydA enzyme, encapsulated in $1\text{--}5\text{ mg mL}^{-1}$ FmocFF and soaked on a carbon felt electrode. Error bars represent mean \pm SD of at least six independent experiments.

self-supporting hydrogel, was formed at $1\text{--}2\text{ mg mL}^{-1}$. Concentrations of $3\text{--}5\text{ mg mL}^{-1}$ produced a stable gel, with visibly increasing turbidity, correlating to the increase in the peptide concentration. These observations were supported by rheology measurements where $1\text{--}2\text{ mg mL}^{-1}$ samples showed very low storage and loss moduli, indicating their liquid state, while a gel state was indicated for the $3\text{--}5\text{ mg mL}^{-1}$ samples by the higher storage moduli compared to the respective loss moduli (Figure 5B). Protein immobilization within a polymer matrix can be attributed to its physical entrapment between dense fibers.³⁴ As the hydrogel's peptide concentration is decreased, a less dense matrix is anticipated to result in an increase in protein leakage and a subsequent decrease in H_2 production. However, the electrochemical H_2 production was not significantly impacted by matrix density differences among the $3\text{--}5\text{ mg mL}^{-1}$ hydrogel samples, despite variations in turbidity and mechanical properties (Figure 5C). This lack of correlation between matrix density and protein retention suggests that the mechanism of FmocFF retention is not governed by protein entanglement within the fibril mesh. Furthermore, even a decrease in the peptide concentration to 2 mg mL^{-1} , which was insufficient to produce a self-supporting 3D gel state, did not

affect H_2 production (Figure 5C). It was only when the peptide concentration was lowered to 1 mg mL^{-1} that a substantial decrease in H_2 production was observed. These results imply that the FmocFF retention mechanism is not directly tied to the presence of a self-supporting 3D gel state or its properties, but rather on reaching a critical concentration of self-assembled fibrils, above which adequate retention is achieved.

3.6 | FmocFF fibrils directly glue protein to carbon fibers

To better understand the interaction between HydA and FmocFF supramolecular fibrils, Cy5-labeled HydA was encapsulated in FmocFF hydrogels at concentrations of $0\text{--}5\text{ mg mL}^{-1}$, without the presence of carbon felt. The localization of the enzyme was subsequently determined by fluorescent confocal microscopy. As expected, no fluorescent signal could be obtained from solution samples, as the enzyme was not concentrated anywhere in the sample (Figure 6A). In the presence of 1 mg mL^{-1} of FmocFF, some enzyme clusters could be viewed (Figure 6B). Interestingly, 2 mg mL^{-1} of FmocFF produced a distinct fluorescent fibril matrix (Figure 6C). Further increase in

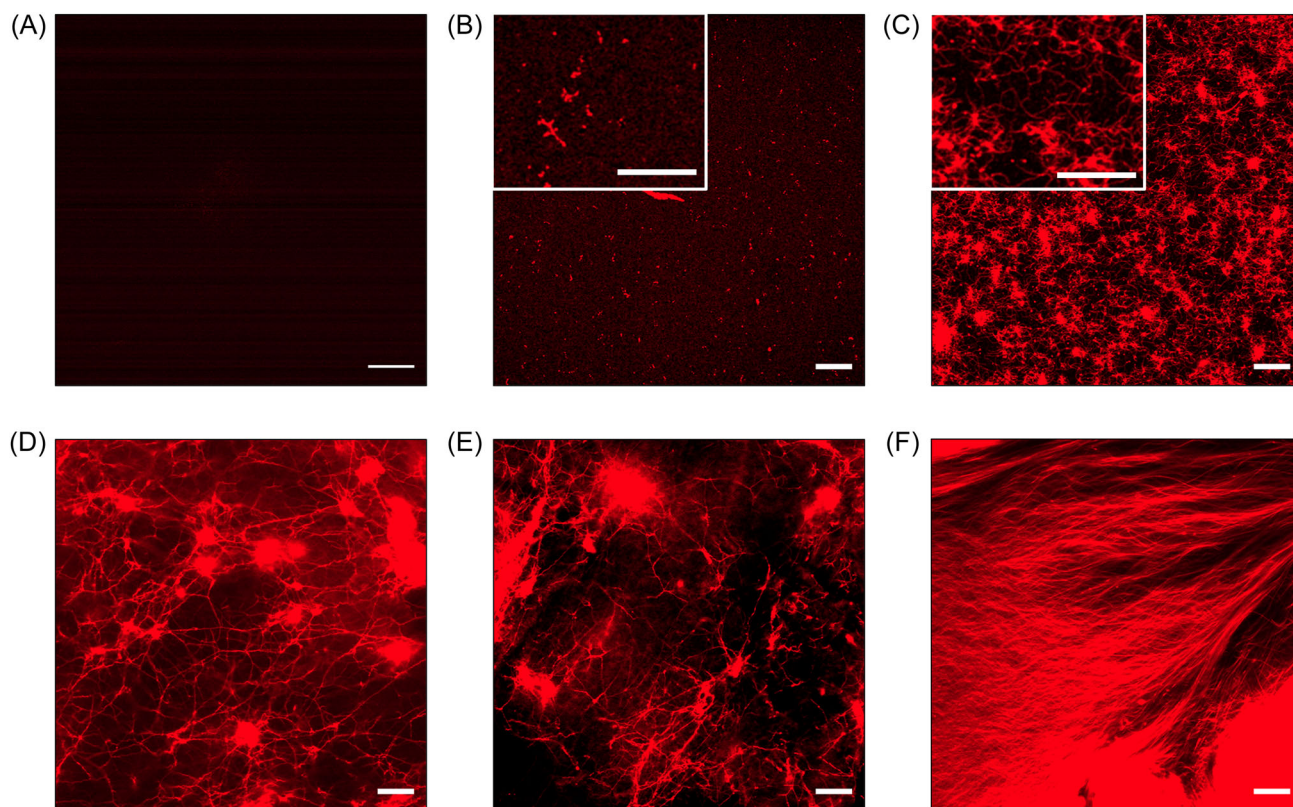


FIGURE 6 HydA distribution within the hydrogel matrix. Confocal microscopy of Cy5-stained HydA with FmocFF at various concentrations. (A) 0 mg mL^{-1} control. (B) 1 mg mL^{-1} . (C) 2 mg mL^{-1} . (D) 3 mg mL^{-1} . (E) 4 mg mL^{-1} . (F) 5 mg mL^{-1} . Scale bar = $10\text{ }\mu\text{m}$.

FmocFF concentrations to 3–5 mg mL⁻¹ resulted in a visible matrix of large fluorescent clusters with interconnecting fibrils (Figure 6D–F).

The visualization of the fluorescent enzyme as a distinct fibril matrix implies direct interaction with the peptide supramolecular structure. These observations are also in line with the H₂ production measured at different FmocFF concentrations (Figure 5C), further supporting the hypothesis of direct protein–FmocFF interaction. In light of this, the clusters viewed at 1 mg mL⁻¹ FmocFF can be interpreted as interaction between the protein and small supramolecular structures, insufficient to retain the enzyme on the carbon felt electrode. This interaction may be attributed to physical adsorption, a common immobilization mechanism in which the enzyme adsorbs to the polymer by van der Waals forces, hydrogen bonds, and ionic and hydrophobic interactions. However, such immobilization is prone to enzyme leakage due to the relatively weak nature of the forces in play. Nonetheless, the interaction between HydA and FmocFF appeared to be strong enough, not only to prevent passive diffusion out of the electrode but also to retain the enzyme in place when potential is applied. When considering physical interactions, π – π and cation– π are among the strongest known, comparable to hydrogen bonds and ion pairing.⁵⁷ The demonstrated strong retention of HydA in FmocFF compared to FmocLL may simply stem from the fewer aromatic

rings of FmocLL and the consequent lower probability for aromatic interactions (Figure 2). A difference in the peptides' supramolecular arrangements could also contribute to this phenomenon, as the assembled FmocLL may expose fewer of the peptide's aromatic, amine, and hydroxyl groups, rendering the assembled fibril less prone to interact with the protein's available residues. Notably, binding of protein to peptide fibrils cannot fully account for retention in carbon felt electrodes. To achieve such retention, the enzyme–fibril complex must also attach to the carbon felt and remain inside it throughout the electrochemical activation. We initially hypothesized the hydrogel fibril matrix to be distributed homogeneously and fill the spaces between the carbon fibers as well as encapsulate HydA in their fibril mesh. While the results obtained with Cy5-labeled HydA encapsulated in FmocLL support this hypothesis, when encapsulated in FmocFF, the labeled HydA was accumulated directly on the carbon fibers, suggesting that the FmocFF fibrils directly interact with the carbon felt (Figure 4C). This difference can arise from FmocLL lacking the available hydrophobic motifs to achieve a strong adherence to the carbon. In addition, a physical mechanism could play a role in FmocFF retention ability as its fibrils appear to be physically entangled around the carbon fibers. Indeed, high-resolution SEM images showed that hydrogel masses directly adhered onto the carbon fibers in FmocFF-soaked carbon felt (Figure 7A).

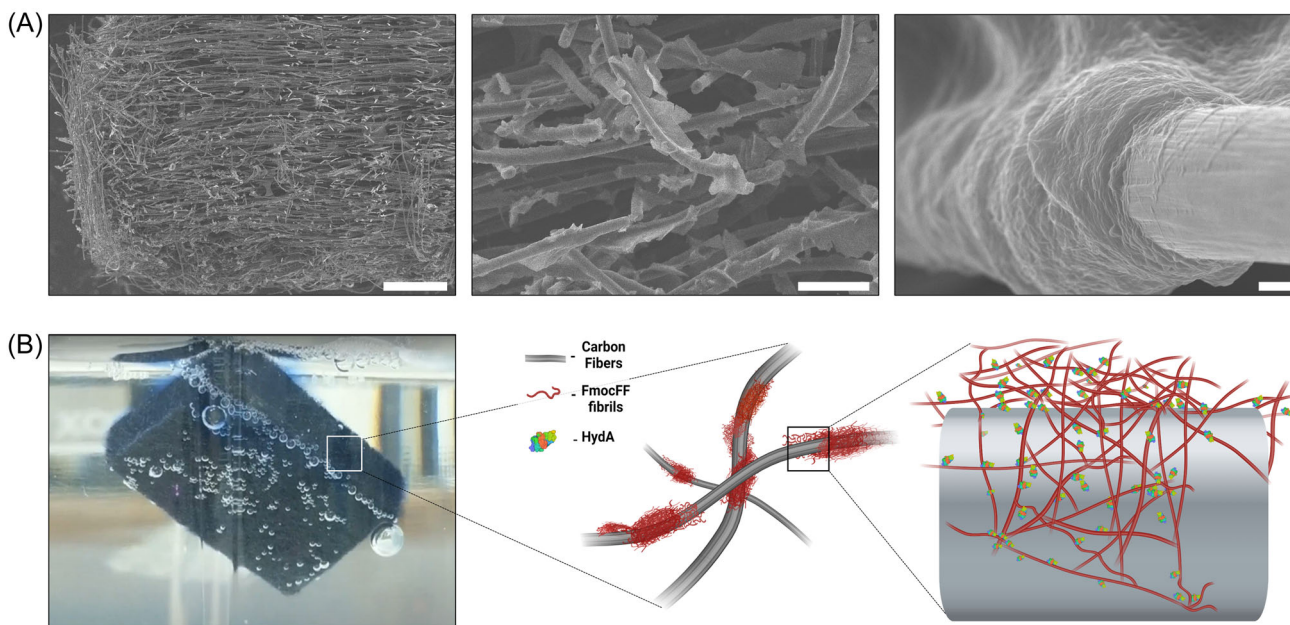


FIGURE 7 FmocFF suggested mode of encapsulation. (A) Scanning electron microscopy images of carbon felt soaked with the FmocFF hydrogel. From left to right—magnifications of $\times 40$, $\times 450$, and $\times 5500$. Respective scale bars are 500, 50, and 2 μm . (B) Illustration of the proposed model. Left—image of a H₂-producing working electrode, composed of a carbon felt soaked with the FmocFF hydrogel encapsulating HydA. Middle—carbon felt fibers are coated with the self-assembled FmocFF fibrils. Right—enzyme molecules are attached to the FmocFF fibrils and thus immobilized over the carbon fibers.

Taking together the interaction of FmocFF with HydA and with the carbon felt, we propose a mode of encapsulation in which FmocFF fibrils act as a glue, binding the protein to the electrode to achieve significantly improved retention, strong enough to resist the electrophoresis forces taking place under the tested experimental conditions (Figure 7B). This model can also explain why the 2 mg mL^{-1} suspensions show strong retention ability even as a liquid.

3.7 | Peptide self-assembly in the presence of HydA improves the enzyme retention efficiency

To further establish the proposed model, we tested whether it is necessary to initiate the self-assembly of FmocFF fibrils in the presence of HydA and carbon felt to achieve the observed efficient retention. We therefore utilized the liquid state of self-assembled FmocFF at 2 mg mL^{-1} to prepare a fibril suspension before HydA introduction and carbon felt soaking. FmocFF was allowed to self-assemble overnight, and HydA was subsequently added to the suspension. The mixture was then incubated for 2 h to allow the enzyme to interact with the assembled FmocFF fibrils before carbon felt soaking. The results show that electrochemical H_2 production measurements were approximately 60% higher in samples where the fibrils were coassembled in the presence of HydA and carbon felt (FmocFF^{mix}), in comparison to samples where FmocFF was preassembled separately (FmocFF^{sep}). Nevertheless, FmocFF^{sep} samples showed 80% higher H_2 production than FmocLL hydrogel samples (Figure 8A). These findings were further supported

by chronoamperometry, which revealed that while the current of FmocFF^{sep} samples decayed faster than that of FmocFF^{mix} samples, the decay was still milder compared to that of FmocLL (Figure 8B). To assess whether these observations correspond to differences in retention ability, an immunoblot assay was conducted as described above. While no detectable band was found in the electrolyte sample of FmocFF^{mix}, a strong detectable HydA band was observed in both FmocLL and FmocFF^{sep} electrolyte samples, implying enzyme loss. Notably, the FmocFF^{sep} band appears to be stronger than that of FmocLL, which contrasts with the higher current and H_2 production obtained from FmocFF^{sep}. However, in this case, the immunoblot assay was not designed to be quantitative; therefore, numerous factors can affect the visualized protein abundance.⁵⁸ Hence, the presence or absence of protein should be considered, rather than the strength of the band, which should be done with care. Nonetheless, based on the higher current and H_2 production compared to FmocLL, it is safe to assume at least partial protein retention by the assembled fibrils of FmocFF^{sep} (Figure 8C). These results suggest that while the presence of all the components upon assembly initiation is not an absolute requisite, it significantly augments enzyme retention. It is possible that initiating the assembly of FmocFF fibrils within the carbon felt results in better adherence of the fibrils to the carbon fibers, which increases the retention strength. Alternatively, the interaction between the FmocFF fibrils and the protein may be more efficient when the enzyme is present during fibril assembly. Nonetheless, the ability to introduce the components separately, while still preserving some retention ability, provides greater flexibility for future applications.

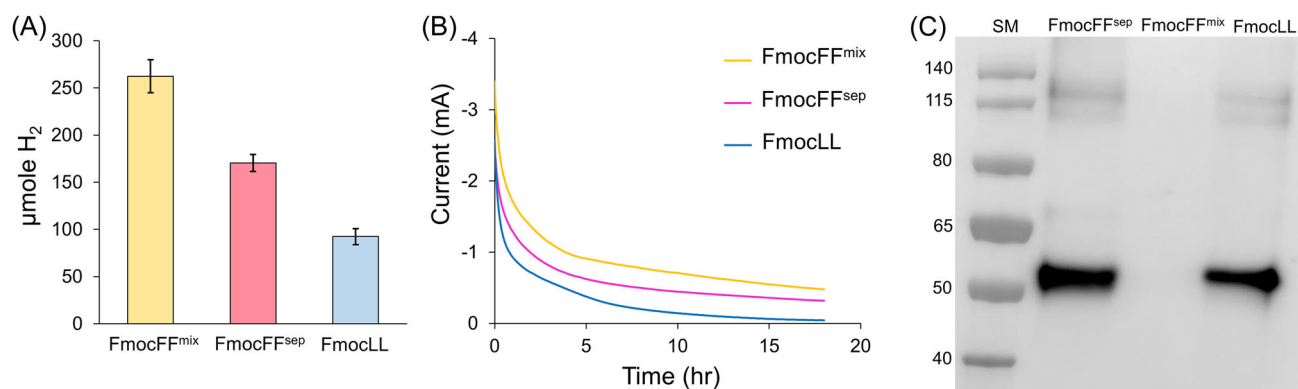


FIGURE 8 Effect of hydrogel self-assembly on HydA retention. (A) H_2 accumulated from overnight (O.N.) electrochemical activation of the HydA enzyme, encapsulated in FmocFF in the presence of HydA and carbon felt (FmocFF^{mix}), in comparison to samples where HydA was added to FmocFF that was preassembled separately (FmocFF^{sep}), and FmocLL. Error bars represent mean \pm SD of at least six independent experiments. (B) Chronoamperometries of O.N. electrochemical assays of FmocFF^{mix}, FmocFF^{sep}, and FmocLL. (C) Immunoblot of HydA in the electrolyte collected after O.N. electrochemical assays of FmocFF^{mix}, FmocFF^{sep}, and FmocLL.

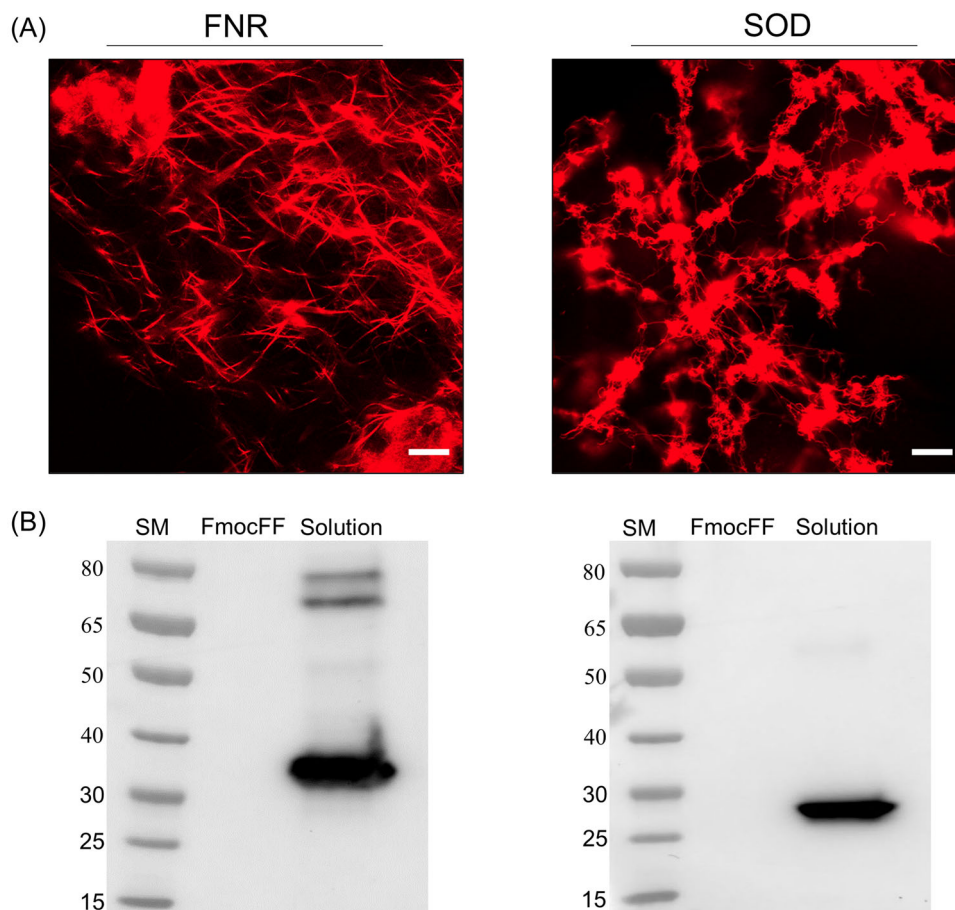


FIGURE 9 FmocFF as an encapsulation platform for other enzymes. (A) Confocal microscopy images of the FmocFF hydrogel with Cy5-labeled FNR (left) and SOD (right); the scale bar is 10 μm . (B) Immunoblot of FNR (left) and SOD (right) collected from the electrolyte after overnight electrochemical assays in the FmocFF hydrogel or solution-soaked electrodes. Specific FNR or SOD antibodies were used for the respective immunoblots.

3.8 | FmocFF could serve as a platform for efficient encapsulation of other proteins for electrochemistry

Finally, we evaluated the generality of protein–fibril interaction by encapsulating two other Cy5-labeled redox enzymes, FNR and SOD, in 3 mg mL⁻¹ FmocFF hydrogel. Similar to HydA-containing hydrogels, the encapsulation of stained FNR and SOD resulted in a fluorescent fibril matrix (Figure 9A). In addition, we assessed the retention ability of FNR and SOD in the FmocFF hydrogel, when subjected to an electrochemical assay. For this purpose, we encapsulated 200 μg of either FNR or SOD together with 75 μg of HydA in FmocFF hydrogels, which were soaked on carbon felt electrodes. Notably, the electrochemical profile obtained by cyclic voltammetry of electrodes supplemented with MV and either FNR or SOD was similar to that obtained with MV-only loaded electrodes (Figure S5). Following overnight electrochemical activation, an immunoblot assay was conducted to detect protein presence in the electrolyte. As

expected, a specific protein band was observed for solution-soaked electrodes, demonstrating the inability of the carbon felt alone to retain the proteins. However, FmocFF-soaked electrodes successfully retained both HydA and FNR or SOD, with no detectable protein bands (Figure 9B). The similar structure and function observed for the three proteins examined suggest a general phenomenon of FmocFF fibril–protein interaction. Hence, this phenomenon may be exploited for encapsulation of other proteins in a variety of electrochemical applications for energy, sensors, bionics, and electrochemical synthesis.

4 | CONCLUSION

We demonstrated that an enzyme encapsulation approach using self-assembled supramolecular structures is effective in 3D electrode settings. The supramolecular structures interact with the enzymes while adhering to the carbon fibers, and hence couple them together to

achieve excellent retention. The ability to retain the enzyme in place while applying electric potential enabled us to utilize a 3D carbon felt electrode to load high amounts of biocatalysts, resulting in high product yield. This arrangement also mitigates diffusion limitations of the electron mediator by localizing the catalysts adjacent to the conductive surface. The ease of immobilization and mild conditions make this method attractive for a variety of biocatalysts, and it can also be applied in processes not related to electrochemistry.

AUTHOR CONTRIBUTIONS

Itzhak Grinberg and **Oren Ben-Zvi**: conceptualization, methodology, investigation, validation, formal analysis, writing—original draft, visualization, writing—review and editing. **Iftach Yacoby** and **Lihl Adler-Abramovich**: Conceptualization, resources, writing—original draft, writing—review and editing, visualization, supervision, project administration, funding acquisition.

ACKNOWLEDGMENTS

The authors are grateful to the members of the Adler-Abramovich and Yacoby laboratories for helpful discussions. The authors gratefully acknowledge Prof. Niyazi Serdar Sariciftci for hosting Itzhak Grinberg for a visit at the Johannes Kepler University and for valuable discussions. The authors are grateful to Yoav Dan for assistance with enzyme labeling and confocal microscopy analysis. The authors acknowledge the Chaoul Center for Nano-scale Systems of Tel Aviv University and the ADAMA Center for Novel Delivery Systems in Crop Protections for the use of instruments and staff assistance. This work was partially supported by funding from the Israel Science Foundation petroleum alternatives to transportation grant (GA 2185/17), and the Israel Ministry of Energy 219-11-120 and 222-11-065. Figures 1, 3A, and 7B were created using [BioRender.com](https://www.biorender.com).

CONFLICT OF INTEREST STATEMENT

The authors declare that there are no conflict of interests.

DATA AVAILABILITY STATEMENT

The data that support the findings of this study are available from the corresponding author upon reasonable request.

ORCID

Itzhak Grinberg  <http://orcid.org/0000-0002-2298-5416>

Oren Ben-Zvi  <https://orcid.org/0000-0001-8672-5923>

Lihl Adler-Abramovich  <https://orcid.org/0000-0003-3433-0625>

Iftach Yacoby  <http://orcid.org/0000-0003-0177-0624>

REFERENCES

- Cavaliere PD, Perrone A, Silvello A. Water electrolysis for the production of hydrogen to be employed in the ironmaking and steelmaking industry. *Metals*. 2021;11(11):1816.
- Zhou D, Li P, Xu W, et al. Recent advances in non-precious metal-based electrodes for alkaline water electrolysis. *ChemNanoMat*. 2020;6(3):336-355.
- Khan MA, Zhao H, Zou W, et al. Recent progresses in electrocatalysts for water electrolysis. *Electrochem Energy Rev*. 2018;1(4):483-530.
- Cracknell JA, Vincent KA, Armstrong FA. Enzymes as working or inspirational electrocatalysts for fuel cells and electrolysis. *Chem Rev*. 2008;108(7):2439-2461.
- Lubitz W, Ogata H, Rüdiger O, Reijerse E. Hydrogenases. *Chem Rev*. 2014;114(8):4081-4148.
- Fourmond V, Baffert C, Sybirna K, et al. The mechanism of inhibition by H₂ of H₂-evolution by hydrogenases. *Chem Commun*. 2013;49(61):6840-6842.
- Rodríguez-Maciá P, Breuer N, Debeer S, Birrell JA. Insight into the redox behavior of the [4Fe-4S] subcluster in [FeFe] hydrogenases. *ACS Catal*. 2020;10(21):13084-13095.
- Morra S, Valetti F, Sarasso V, Castrignanò S, Sadeghi SJ, Gilardi G. Hydrogen production at high Faradaic efficiency by a bio-electrode based on TiO₂ adsorption of a new [FeFe]-hydrogenase from *Clostridium perfringens*. *Bioelectrochemistry*. 2015;106:258-262.
- McDonald TJ, Svedruzic D, Kim YH, et al. Wiring-up hydrogenase with single-walled carbon nanotubes. *Nano Lett*. 2007;7(11):3528-3534.
- Kihara T, Liu XY, Nakamura C, et al. Direct electron transfer to hydrogenase for catalytic hydrogen production using a single-walled carbon nanotube forest. *Int J Hydrogen Energy*. 2011;36(13):7523-7529.
- Léger C, Bertrand P. Direct electrochemistry of redox enzymes as a tool for mechanistic studies. *Chem Rev*. 2008;108(7):2379-2438.
- Gates AJ, Kemp GL, To CY, et al. The relationship between redox enzyme activity and electrochemical potential—cellular and mechanistic implications from protein film electrochemistry. *Phys Chem Chem Phys*. 2011;13(17):7720-7731.
- Kahoush M, Behary N, Guan J, Cayla A, Mutel B, Nierstrasz V. Genipin-mediated immobilization of glucose oxidase enzyme on carbon felt for use as heterogeneous catalyst in sustainable wastewater treatment. *J Environ Chem Eng*. 2021;9(4):105633.
- Downard AJ. Electrochemically assisted covalent modification of carbon electrodes. *Electroanalysis*. 2000;12(14):1085-1096.
- Guan D, Kurra Y, Liu W, Chen Z. A click chemistry approach to site-specific immobilization of a small laccase enables efficient direct electron transfer in a biocathode. *Chem Commun*. 2015;51(13):2522-2525.
- Onoda A, Inoue N, Campidelli S, Hayashi T. Cofactor-specific covalent anchoring of cytochrome: B562 on a single-walled carbon nanotube by click chemistry. *RSC Adv*. 2016;6(70):65936-65940.
- Yates NDJ, Fascione MA, Parkin A. Methodologies for “wiring” redox proteins/enzymes to electrode surfaces. *Chem Eur J*. 2018;24(47):12164-12182.

18. Michaelis L, Hill ES. The viologen indicators. *J Gen Physiol.* 1933;16(6):859-873.
19. Tatsumi H, Takagi K, Fujita M, Kano K, Ikeda T. Electrochemical study of reversible hydrogenase reaction of *Desulfovibrio vulgaris* cells with methyl viologen as an electron carrier. *Anal Chem.* 1999;71(9):1753-1759.
20. Lojou E, Giudici-Ortoni M, Bianco P. Direct electrochemistry and enzymatic activity of bacterial polyhemic cytochrome c3 incorporated in clay films. *J Electroanal Chem.* 2005;579(2):199-213.
21. Cadoux C, Milton RD. Recent enzymatic electrochemistry for reductive reactions. *ChemElectroChem.* 2020;7(9):1974-1986.
22. Plumeré N, Rüdiger O, Oughli AA, et al. A redox hydrogel protects hydrogenase from high-potential deactivation and oxygen damage. *Nat Chem.* 2014;6(9):822-827.
23. Ruth JC, Milton RD, Gu W, Spormann AM. Enhanced electrosynthetic hydrogen evolution by hydrogenases embedded in a redox-active hydrogel. *Chem Eur J.* 2020;26(32):7323-7329.
24. Castañeda-Losada L, Adam D, Paczia N, et al. Bioelectrocatalytic cofactor regeneration coupled to CO₂ fixation in a redox-active hydrogel for stereoselective C–C bond formation. *Angew Chem Int Ed.* 2021;60(38):21056-21061.
25. Li H, Buesen D, Dementin S, Léger C, Fourmond V, Plumeré N. Complete protection of O₂-sensitive catalysts in thin films. *J Am Chem Soc.* 2019;141(42):16734-16742.
26. Mersch D, Lee CY, Zhang JZ, et al. Wiring of photosystem II to hydrogenase for photoelectrochemical water splitting. *J Am Chem Soc.* 2015;137(26):8541-8549.
27. Chen X, Lawrence JM, Wey LT, et al. 3D-printed hierarchical pillar array electrodes for high-performance semi-artificial photosynthesis. *Nat Mater.* 2022;21(7):811-818.
28. Sun H, Zhu J, Baumann D, et al. Hierarchical 3D electrodes for electrochemical energy storage. *Nat Rev Mater.* 2019;4(1):45-60.
29. Healy AJ, Reeve HA, Parkin A, Vincent KA. Electrically conducting particle networks in polymer electrolyte as three-dimensional electrodes for hydrogenase electrocatalysis. *Electrochim Acta.* 2011;56(28):10786-10790.
30. Baur J, Le Goff A, Dementin S, Holzinger M, Rousset M, Cosnier S. Three-dimensional carbon nanotube-polypyrrole-[NiFe] hydrogenase electrodes for the efficient electrocatalytic oxidation of H₂. *Int J Hydrogen Energy.* 2011;36(19):12096-12101.
31. Mohamad NR, Marzuki NHC, Buang NA, Huyop F, Wahab RA. An overview of technologies for immobilization of enzymes and surface analysis techniques for immobilized enzymes. *Biotechnol Biotechnol Equip.* 2015;29(2):205-220.
32. Schlager S, Fuchsbaauer A, Haberbaauer M, Neugebauer H, Sariciftci NS. Carbon dioxide conversion to synthetic fuels using biocatalytic electrodes. *J Mater Chem A.* 2017;5(6):2429-2443.
33. Shiraiwa S, So K, Sugimoto Y, et al. Reactivation of standard [NiFe]-hydrogenase and bioelectrochemical catalysis of proton reduction and hydrogen oxidation in a mediated-electron-transfer system. *Bioelectrochemistry.* 2018;123:156-161.
34. Rodriguez-Abetxuko A, Sánchez-deAlcázar D, Muñumer P, Belouqui A. Tunable polymeric scaffolds for enzyme immobilization. *Front Bioeng Biotechnol.* 2020;8:830.
35. Varga M. Self-assembly of nanobiomaterials. In: Grumezescu AM, ed. *Fabrication and Self-Assembly of Nanobiomaterials: Applications of Nanobiomaterials.* William Andrew Publishing; 2016:57-90.
36. Seelbach RJ, Franssen P, Pulido D, et al. Injectable hyaluronan hydrogels with peptide-binding dendrimers modulate the controlled release of BMP-2 and TGF- β 1. *Macromol Biosci.* 2015;15(8):1035-1044.
37. Smith KH, Tejada-Montes E, Poch M, Mata A. Integrating top-down and self-assembly in the fabrication of peptide and protein-based biomedical materials. *Chem Soc Rev.* 2011;40(9):4563-4577.
38. Fichman G, Gazit E. Self-assembly of short peptides to form hydrogels: design of building blocks, physical properties and technological applications. *Acta Biomater.* 2014;10(4):1671-1682.
39. Fleming S, Ulijn RV. Design of nanostructures based on aromatic peptide amphiphiles. *Chem Soc Rev.* 2014;43(23):8150-8177.
40. Mahler A, Reches M, Rechter M, Cohen S, Gazit E. Rigid, self-assembled hydrogel composed of a modified aromatic dipeptide. *Adv Mater.* 2006;18(11):1365-1370.
41. Jayawarna V, Ali M, Jowitt TA, et al. Nanostructured hydrogels for three-dimensional cell culture through self-assembly of fluorenylmethoxycarbonyl-dipeptides. *Adv Mater.* 2006;18(5):611-614.
42. Schnaider L, Toprakcioglu Z, Ezra A, et al. Biocompatible hybrid organic/inorganic microhydrogels promote bacterial adherence and eradication in vitro and in vivo. *Nano Lett.* 2020;20(3):1590-1597.
43. Zhang S. Discovery and design of self-assembling peptides. *Interface Focus.* 2017;7(6):20170028.
44. Muller C, Ontani A, Bigo-Simon A, Schaaf P, Jerry L. Localized enzyme-assisted self-assembly of low molecular weight hydrogelators. Mechanism, applications and perspectives. *Adv Colloid Interface Sci.* 2022;304:102660.
45. Rodon Fores J, Bigo-Simon A, Wagner D, et al. Localized enzyme-assisted self-assembly in the presence of hyaluronic acid for hybrid supramolecular hydrogel coating. *Polymers.* 2021;13(11):1793.
46. Li Q, Zhang G, Wu Y, et al. Control of peptide hydrogel formation and stability via heating treatment. *J Colloid Interface Sci.* 2021;583:234-242.
47. Bellotto O, Kralj S, De Zorzi R, Geremia S, Marchesan S. Supramolecular hydrogels from unprotected dipeptides: a comparative study on stereoisomers and structural isomers. *Soft Matter.* 2020;16(44):10151-10157.
48. Panda JJ, Chauhan VS. Short peptide based self-assembled nanostructures: implications in drug delivery and tissue engineering. *Polym Chem.* 2014;5(15):4431-4449.
49. Hauser CAE, Zhang S. Designer self-assembling peptide nanofiber biological materials. *Chem Soc Rev.* 2010;39(8):2780-2790.
50. Dudukovic NA, Zukoski CF. Mechanical properties of self-assembled Fmoc-diphenylalanine molecular gels. *Langmuir.* 2014;30(15):4493-4500.
51. Orbach R, Adler-Abramovich L, Zigerson S, Mironi-Harpaz I, Seliktar D, Gazit E. Self-assembled Fmoc-peptides as a

- platform for the formation of nanostructures and hydrogels. *Biomacromolecules*. 2009;10(9):2646-2651.
52. Orbach R, Mironi-Harpaz I, Adler-Abramovich L, et al. The rheological and structural properties of Fmoc-peptide-based hydrogels: the effect of aromatic molecular architecture on self-assembly and physical characteristics. *Langmuir*. 2012; 28(4):2015-2022.
 53. Adler-Abramovich L, Gazit E. The physical properties of supramolecular peptide assemblies: from building block association to technological applications. *Chem Soc Rev*. 2014;43(20):6881-6893.
 54. Ben-Zvi O, Grinberg I, Orr AA, et al. Protection of oxygen-sensitive enzymes by peptide hydrogel. *ACS Nano*. 2021;15(4): 6530-6539.
 55. Ben-Zvi O, Yacoby I. The in-vitro enhancement of FeFe hydrogenase activity by superoxide dismutase. *Int J Hydrogen Energy*. 2016;41(39):17274-17282.
 56. Marco P, Elman T, Yacoby I. Binding of ferredoxin NADP⁺ oxidoreductase (FNR) to plant photosystem I. *Biochim Biophys Acta Bioenergy*. 2019;1860(9):689-698.
 57. Yacoby I, Tegler LT, Pochekailov S, Zhang S, King PW. Optimized expression and purification for high-activity preparations of algal [FeFe]-hydrogenase. *PLoS One*. 2012; 7(4):e35886.
 58. Silakov A, Kamp C, Reijerse E, Happe T, Lubitz W. Spectro-electrochemical characterization of the active site of the [FeFe] hydrogenase HydA1 from *Chlamydomonas reinhardtii*. *Biochemistry*. 2009;48(33):7780-7786.
 59. Frederix PWJM, Kania R, Wright JA, et al. Encapsulating [FeFe]-hydrogenase model compounds in peptide hydrogels dramatically modifies stability and photochemistry. *Dalton Trans*. 2012;41(42):13112-13119.
 60. Dougherty DA. The cation- π interaction. *Acc Chem Res*. 2013;46(4):885-893.
 61. Pillai-Kastoori L, Schutz-Geschwender AR, Harford JA. A systematic approach to quantitative Western blot analysis. *Anal Biochem*. 2020;593:113608.

SUPPORTING INFORMATION

Additional supporting information can be found online in the Supporting Information section at the end of this article.

How to cite this article: Grinberg I, Ben-Zvi O, Adler-Abramovich L, Yacoby I. Peptide self-assembly as a strategy for facile immobilization of redox enzymes on carbon electrodes. *Carbon Energy*. 2023;e411. doi:10.1002/cey2.411